International Journal of Signal Processing, Image Processing and Pattern Recognition
Vol.9, No.12, (2016), pp.243-250
http://dx.doi.org/10.14257/ijsip.2016.9.12.23

An Improved Algorithm for Acoustic Radiation Force Impulse Imaging Based on Loupas Approach

YouXin, ShiDan, YinHao, LiuYu and Dongc Liu

Sichuan University，Medical imaging Lab, Sichuan, Chengdu
tingfengyx@sina.com

Abstract

With the purpose of solving the issue that there are errors in the traditional Loupas Algorithm used in ARFI and the effects of imaging are not as good as expected, this thesis will talk about an improved method to solve this proplem.Based on Loupas Algorithm, it is presented that we can get more accurate computing result of the displacement by changing the size of the sampling time windows and calculating the average speed according to the 2D autocorrelator.The method presented in this paper is aimed at doing computing refering to the tiny displacement caused by the push from ARFI and comparing between the displacement-time graph of the focus of the windows with different value.Finally,from these,people can know the most suitable value of the sampling time windows.Compared with the result of the experientunder traditional Loupas Algorithm,that of this experient has improved a lot.As a result,not only Elastographic Contrast-to-Noise Ratio has been improved,but also the image quality.

Keywords:*ARFI;Elasticity Imaging; 2D Autocorrelator Algorithm; Sampling Time Windows*

1. Introduction

Vibration Sonoelastography was invented by Fatemi and Greenleaf in 1998.This technology uses an ultrasonic field to produce a low-frequency vibration and to work on the examined tissues.And then,according to the elastic modulus of itself,the tissues cause different amplitude vibration.Finally,it displays the result through images. [1-2] The acoustic radiation force impulse imaging which uses ARFI is a kind of Vibration Sonoelastography.ARFI imaging measures tissue responses by using radiation force from long pulses to impart localized displacements in order to gain insight into the local viscoelastic properties of soft tissue in vivo and in vitro [3-4].As the basis of the analysis of tissue biomechanics characteristic, the displacement estimation is the most important tache of ARFI.Typically performed using cross-correlation method ,Iterative phase zero method or loupas Algor`ithm,an estimate of tissue displacement can be made between signals collected before the excitation (reference) and after the excitation (tracking) [5]. The cross-correlation technique measures the similarity between a windowed length of data from the reference and tracking signals [6];Iterative phase zero method is a kind of displacement estimation algorithms based on the phase domain presented by Andreas Pesavento in 1999. It applies Newton's Method to the phase zero method and gets the estimation results of the present sampling point by computing the iteration of the estimation results of time delay [7]. loupas Algorithm provides a velocity estimator which is the derivation of axial velocity values by evaluating the Doppler equation using explicit estimates of both the mean Doppler and the mean RF frequency at each range gate location [8]. Loupas combines the generally higher performance of 2D broadband time-domain techniques with the relatively modest complexity of 1D narrowband

ISSN: 2005-4254 IJSIP

phase-domain velocity estimators meets computational requirements of the proposed estimator.

Nowadays,Acoustic Radiation Force Impluse Imaging usually uses Loupas Algorithm to get the small displacement caused by Acoustic Radiation Force.However,in the traditional Loupas Algorithm,it usually chooses different sampling point in different time from the beginning to the end to carry on the calculation of absolute displacement. By using this computing method,the value of N on the windows of time is 2, which is easily influenced by noise.And as a result,the displacement curve can't be unbroken or smoothing.Concretely speaking, because the value for sampling window N is small(for the minimum 2), calculation time of echo phase displacement is too short and there is great error in the calculation.It can be told from the three part of displacement curve that the calculation result trembles, which causes that the imaging result is not as good as expected.While when the value of N is too big, calculation time of echo phase displacement is too long and there are too many useless information, which causes that the calculation result can’t be accurate enough and the imaging result is not so good.This thesis focus on comparing echo displacement-time curve of focal area of different sampling time window in the process of imaging,choosing appropriate value of sampling time window and feeds back optimized parameters to the system so as to achieve better image effect.

2. Methods

2.1. Algorithm Methods

The mean velocity obtained from the 2D autocorrelator for the case of the complex demodulated signal $z(\mathrm{m},\mathrm{n})$ [8]:

$$\left\langle \upsilon_{2\mathrm{D}} \right\rangle = \frac{ct_s \left\langle F \right\rangle}{2T_s \left\langle f \right\rangle} \cong \frac{c}{2} \frac{\frac{1}{2\pi T_s} \tan^{-1}\left\{ \frac{\mathrm{Im}\left[\gamma_{dem}(0,1)\right]}{\mathrm{Re}\left[\gamma_{dem}(0,1)\right]} \right\}}{\frac{1}{2\pi t_s}\left(2\pi f_{dem} + \tan^{-1}\left\{ \frac{\mathrm{Im}\left[\gamma_{dem}(0,1)\right]}{\mathrm{Re}\left[\gamma_{dem}(0,1)\right]} \right\} \right)} \tag{1}$$

where γ_{dem} is the 2D autocorrelation function of $z(\mathrm{m},\mathrm{n})$

$$\begin{aligned}\gamma_{dem}(m',n') &= \sum_{m=0}^{M-m'-1} \sum_{n=0}^{N-n'-1} z(m,n) z^*(m+m',n+n') \\ &= \sum_{m=0}^{M-m'-1} \sum_{n=0}^{N-n'-1} \left[I(m,n) I(m+m',n+n') + Q(m,n) Q(m+m',n+n') \right] \\ &\quad + j \sum_{m=0}^{M-m'-1} \sum_{n=0}^{N-n'-1} \left[Q(m,n) I(m+m',n+n') - I(m,n) Q(m+m',n+n') \right]\end{aligned}$$

(2)

Finally,(1) and (2)can be combined to express the mean velocity in terms of the I $\&Q$ samples according to (3).

$$\left\langle \upsilon_{2D} \right\rangle \cong \frac{c}{2} \frac{\frac{1}{2\pi T_s}\tan^{-1}\left\{\frac{\sum_{m=0}^{M-1}\sum_{n=0}^{N-2}\left[Q(m,n)I(m,n+1)-I(m,n)Q(m,n+1)\right]}{\sum_{m=0}^{M-1}\sum_{n=0}^{N-2}\left[I(m,n)I(m,n+1)+Q(m,n)Q(m,n+1)\right]}\right\}}{\frac{1}{2\pi t_s}\left(2\pi f_{dem}+\tan^{-1}\left\{\frac{\sum_{m=0}^{M-2}\sum_{n=0}^{N-1}\left[Q(m,n)I(m+1,n)-I(m,n)Q(m+1,n)\right]}{\sum_{m=0}^{M-2}\sum_{n=0}^{N-1}\left[I(m,n)I(m+1,n)+Q(m,n)Q(m+1,n\right]}\right\}\right)} \quad (3)$$

2.2. Average Displacement Calculation

Involving the use of Loupas to compute ARFI displacement in earlier literature, the value of sampling time window is used to be 2, echo signal produced by the pushing beam is removed due to of the interference of long wave emission which make it invalid. We use echo signal corresponding to the reference beam as a benchmark to calculate with the rest of the beams respectively.

Due to requiring to change the sampling time window and guarantee interval consistency between each beam in the direction of time, the signal needs to be resampled before calculating the displacement. In this paper, we use linear interpolation, by means of linear interpolation for adjacent tracking beams to replace 3 pushing beams respectively. Then we use Equation (3) and change the value of N in equation to calculate the average velocity in sampling time window of adjacent beams.Finally,we use Equation (5),(6) to calculate the concrete displacement.

$$\bar{u}_i = \bar{v}_i * T_{PRF} \quad (4)$$

$$\bar{u} = \frac{c}{4\pi f_c} \frac{\tan^{-1}\left\{\frac{\sum_{m=0}^{M-1}\sum_{n=0}^{N-2}\left[Q(m,n)I(m,n+1)-I(m,n)Q(m,n+1)\right]}{\sum_{m=0}^{M-1}\sum_{n=0}^{N-2}\left[I(m,n)I(m,n+1)+Q(m,n)Q(m,n+1)\right]}\right\}}{1+\tan^{-1}\left\{\frac{\sum_{m=0}^{M-2}\sum_{n=0}^{N-1}\left[Q(m,n)I(m+1,n)-I(m,n)Q(m+1,n)\right]}{\sum_{m=0}^{M-2}\sum_{n=0}^{N-1}\left[I(m,n)I(m+1,n)+Q(m,n)Q(m+1,n)\right]}\right\} f_s / 2\pi f_c} \quad (5)$$

$$d_i = d_{i-1} + \bar{u}_i \quad (6)$$

where u_i is local displacement of organization in unit time; f_c is center frequency; f_s is sampling frequency; d_i is local displacement of organization belong time; T_{PRF} is pulse repetition period; i is between 0 and ensemble size; d_0 specify the initial time, and d_0 =0 due to no acoustic radiation force.

3. Results and Discussion

The 2D ARFI images were formed with some lateral pushing locations separated by 0.5 mm, each with the same focal depth. The received echoes from the consecutive tracking beams at each lateral position were correlated with the neighbor beam to calculate the induced displacement by using the algorithm proposed in section2 with I/Q data.

In the ensemble direction, the beam sequence was modified to consist of pushing beams and tracking beams. The first beam was a standard B-mode pulse with 2 cycles, which was used as the reference beam for measuring tissue displacements. The pushing beam was then fired along the same line with 200 cycles and variable voltage control. There are 3 pushing beams within the ensemble size 24, and the beam sequence is described in Figure 1.

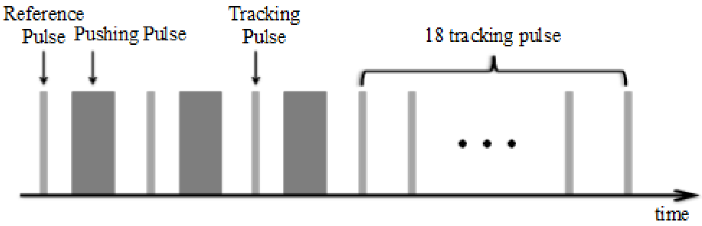

Figure 1. Pulse Sequence Diagram

During experimental data collection, the probe center frequency is 5 MHZ, sampling frequency for 40 MHZ, repetition frequency of 8.88 kHz. We use using Model049 mode for experiments which consists of four different dynamic characteristics of the spherical organization and elasticity background tissue and the elastic coefficient of type 1-4 in the order: 8 kPa, 14 kPa, 45kPa, 80kPa, background region for 25 kPa.In this paper, we use 8kPa type spherical organization for acoustic radiation force pushing and echo detection.

3.1. Displacement -Time Curve Analysis

In this paper, the ensemble size is 24, so the range of sampling time window N in autocorrelation algorithm is between 2 and 24(2≤N≤24). Due to the large N values, interfered with redundant information, experiment results will be inaccurate and calculation efficiency will be reduced, we only select 9 sets of data (2≤N≤10) for studying, and only show the original Loupas algorithm, the values of N for the 4,6,8 to display. By analyzing the algorithm in the Section 2, using autocorrelation algorithm proposed in this paper, we can calculate the tiny displacement in the experimental environment within the selected ROI position caused by acoustic radiation force through Equation (5). Because there is the strongest energy and the most accurate information in focal area of ARFI imaging technology, and in order to facilitate the research on the rules of the displacement caused by acoustic radiation force, we choose the point within valid focal area to calculate and display its average echo displacement -time curve linearly according to Equation (7).

$$r_D = 2 f_{\#}^{2} \lambda \tag{7}$$

where r_D is the length of valid focal area, $f_{\#}$ is the ratio of the focal depth to the aperture width, λ is wave length. In this paper, $f_{\#}$ =1.5, r_D =0.14cm

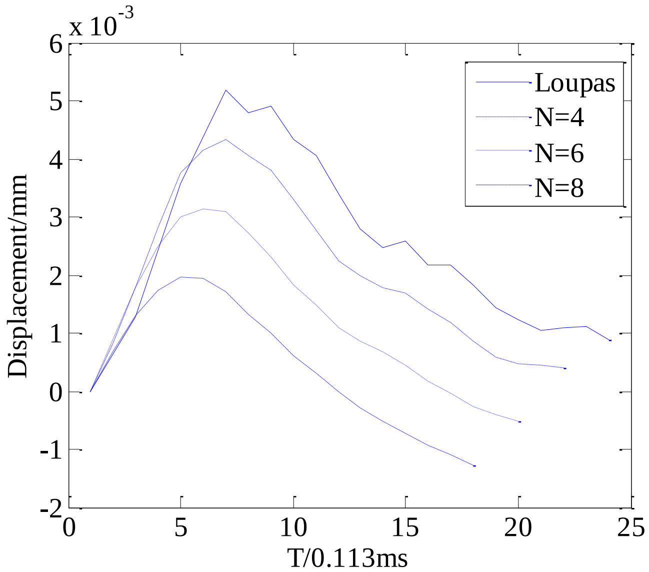

Figure 2. Displacement -Time Curve Within Valid Focal Area

The average echo displacement - time curve within valid focal area of original Loupas algorithm and improved algorithm in different sampling time window size (N = 4, 6, 8) is shown in Figure 2. Because the pushing pulse echo is invalid to be delete in the Loupas algorithm, we use linear interpolation method to replace 3 values corresponding to deleted echo in displacement -time curve. As shown in Figure 2, within the ensemble size, the movement of the balls are almost from 0 to a certain displacement, then tend to be balance. As the value of N increased, displacement curve is smoother.

Where there is negative in the displacement, it explains the ball move backward. However, within the ensemble size, along the time direction, the ball should tend to be balance last moment instead of backward movement, it can be seen from the displacement-time curve calculated using Loupas algorithm. And we can observe the displacement tends to 0 last moment, instead of negative. Therefore, when there is negative in the displacement, it explains the value of N is too large, too much information contained while calculating the displacement, which lead calculated reverse speed too large and inaccurate to result in negative displacement, then makes the final computation results is error.

Therefore, when there is negative in the displacement, the value of N is too large, which makes the calculation result is inaccurate, and reduce the imaging quality finally. As shown in Figure 2, When N = 4, smoothness of curve is highest and at the last the displacement tends to be 0(the ball tends to be balance) instead of negative, so 4 is the most appropriate value for imaging.

3.2. Matlab Simulation of Images and Computational Research

In this paper, for the different sampling time window size, we choose the moment displacement is peak for imaging within the ensemble size respectively, instead choosing fixed moment for imaging as existing medical ultrasound radiation force imaging provided, and compare images with original Loupas algorithm, as shown in Figure 3.

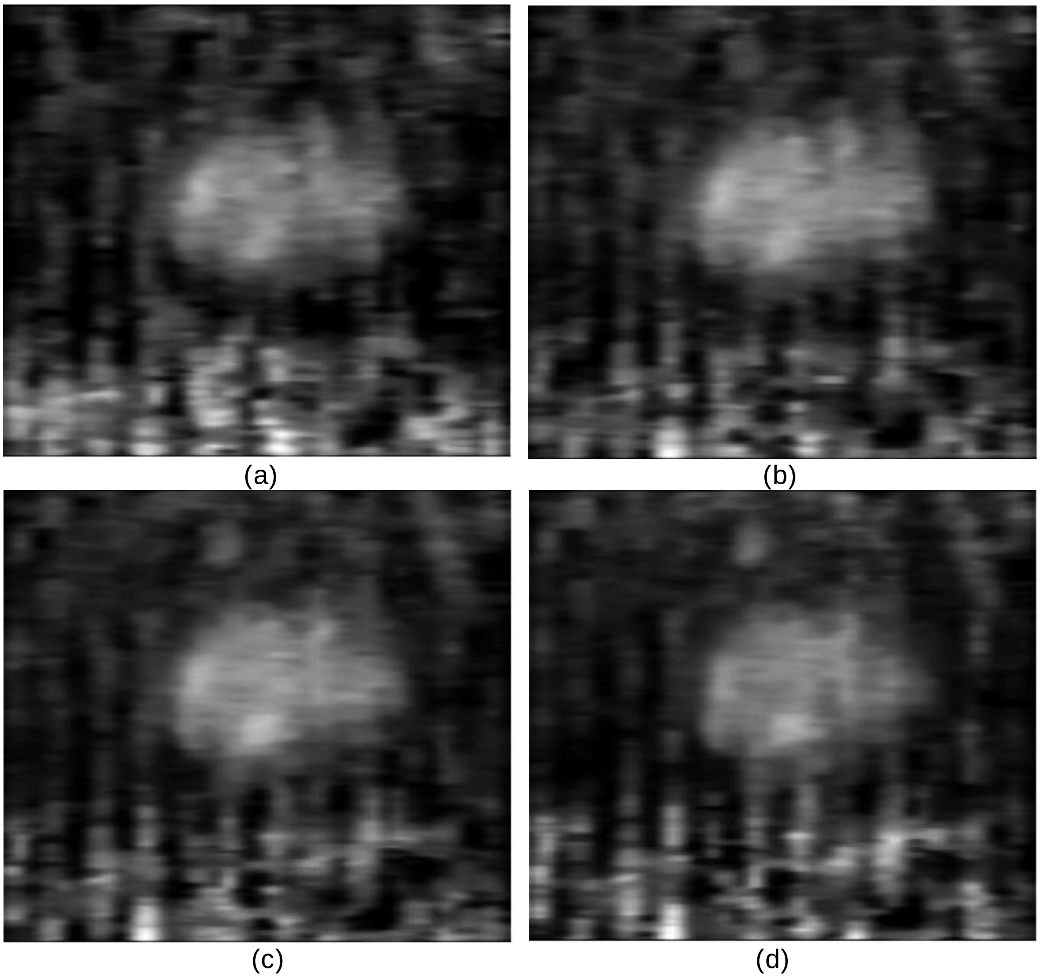

Figure 3. Simulation Images of Loupas Algorithm and Different Values of N.(a) is the Image of Original Loupas Algorithm,(b) to (d) of N=4,6,8 Respectively

We can see when N is small (the original algorithm), the image is not good; when N is too large, imaging quality does not improve with the increase of N, reduced instead; when N=4,the imaging quality is best.

To further confirm the imaging quality is best when N=4, we use Elastographic Contrast-to-Noise Ratio(CNR) [9] and Equation (8) for compare.

$$CNR = \frac{2(\mu_t - \mu_b)^2}{\sigma_t^2 + \sigma_b^2} \tag{8}$$

μ_t and σ_t are the strain mean and standard deviation of the target area respectively; μ_b and σ_b are the strain mean and standard deviation of background area respectively.

We use the area within the ball as target area and 4 areas outside of the ball as background areas to calculate CNR respectively, and then use 4 CNR for averaging (the 5 areas are almost equal).

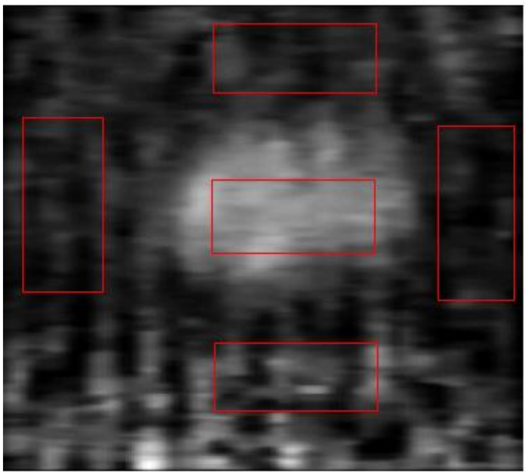

Figure 4. Schematic Diagram of Calculated CNR Region Selection

And results are shown in Table 1:

	Loupas	N=4	N=6	N=8
CNR	4.4077	7.6942	6.5053	4.3537

Table 1. CNR of Simulation Image

We can see when N=4,CNR is the highest, proving that 4 is the best value once again.

4. Conclusion

In this paper, we study the algorithm of acoustic radiation force imaging, and improve the Loupas algorithm which is used for acoustic radiation force imaging now. We use displacement -time curve of focal area center to choose appropriate value of sampling time window of algorithm, in order to achieve better imaging results.

Because the value for sampling time window N is small (for the minimum 2) in Loupas algorithm used now, calculation time of echo phase displacement is too short and there is great error in the calculation, we solve this problem and study the optimal value of the N. By observing the calculated average displacement - time curves of echo under different sampling time window size of effective focal area, we find when the value of N increases to a certain value, there is negative in the displacement which explains the ball produced backward motion. However, within the scope of t sampling volume, along the time direction, the ball should tend to be balance last moment instead of backward movement. This situation explains the value of N is too large, calculation result is so disturbed by too much redundant information that it is inaccurate, imaging quality is reduced finally. At last, we find when the value of sampling time window N takes 4, we can get the best imaging according to displacement -time curve of focal area center, the matlab simulation of images and computational research of CNR.

Using the provided echo displacement detection method based on acoustic radiation force, we can effectively choose suitable sampling time window in the process of displacement detection which make higher displacement detection reliability and better imaging quality. And there is a certain significance to improve the existing medical ultrasound radiation imaging system and provide more accurate results show for the diagnosis. In this paper, we study only for 3 pushing beams within the ensemble size 24 so that it is relatively limited. Follow-up work will study the best values of sampling time window size corresponding to different pushing beams within the ensemble size 24, so that we can adaptively adjust the sampling time window size in the process of displacement detection.

Acknowledgements

We thank Shidan,Yinhao,Dongc Liu for their guidance,and thank Saset Healthcare for their system support.

References

[1] M. Fatemi, J. F. Greenleaf, "Vibro-acoustography: an imaging modality based on ultrasound-stimulated acoustic emission", Proc Natl Acad Sci U S A, vol. 96, no. 12, **(1999)**, pp. 6603-6608.
[2] M. Fatemi and J. F. Greenleaf, "Ultrasound-stimulated vibro-acoustic spectrography", Science, vol. 280, no. 5360, **(1998)**, pp. 82-85.
[3] K Nightangle, R. Bently and G. Trahey, "Observations of Tissue Response to Acoustic Radiation Force:Opportunities for Imaging", Ultrasonic Imaging, vol. 24, no. 3, **(2002)**, pp. 129-138.
[4] K. Nightingale and M. Soo, "Acoustic radiation force impulse imaging: in vivo demonstration of clinical feasibility", Ultrasound in Medicine & Biology, vol. 28, no. 2, **(2002)**, pp. 227-235(9).
[5] J. R. Doherty, G. E. Trahey, K. Nightangle and M. L. Palmeri, "Acoustic radiation force elasticity imaging in diagnostic ultrasound", IEEE Trans Ultrason Ferroelectr Freq Control, vol. 60, no. 4, **(2013)**, pp. 685 - 701.
[6] O. Bonnefous and P. Pesqué, "Time domain formulation of pulse-Doppler ultrasound and blood velocity estimation by cross correlation", Ultrasonic Imaging, vol. 8, no. 2, **(1986)**, pp. 73–85.
[7] A. Pesavento, C. Perrey and M. Krueger, "A time-efficient and accurate strain estimation concept for ultrasonic elastography using iterative phase zero estimation", IEEE Transactions on Ultrasonics, Ferroelectrics, and Frequency Control, vol. 46, no. 5, **(1999)**, pp. 1057 - 1067.
[8] T. Loupas, J. T. Powers and R. W. Gill, "An axial velocity estimator for ultrasound blood flow imaging, based on a full evaluation of the Doppler equation by means of a two-dimensional autocorrelation approach", Ultrasonics Ferroelectrics and Frequency Control, IEEE Transactions on, vol. 42, no. 4, **(1995),** pp. 672 - 688.
[9] S. Cui and D. C. Liu, "Noise Reduction for Ultrasonic Elastography Using Transmit-Side Frequency Compounding: A Preliminary Study", IEEE Trans Ultrason Ferroelec Freq Control, vol. 58, no. 3, **(2011)**.

